IMPLEMENTATION OF A GRID CONNECTED PHOTOVOLTAIC SYSTEM CONTROLLED BY DIGITAL SIGNAL PROCESSOR

G. M. S. Azevedo[1], M. C. Cavalcanti[1], F. A. S. Neves[1], P. Rodriguez[2]
(1) Universidade Federal de Pernambuco (UFPE) - Departamento de Engenharia Elétrica e Sistemas de Potência
Recife, Pernambuco, Brazil, Emails: gustavomsa@netscape.net, marcelo.cavalcanti@ufpe.br, fneves@ufpe.br
(2) Universitat Politècnica de Catalunya (UPC) - Departament d'Enginyeria Elèctrica
Barcelona, Spain, Email: prodriguez@ee.upc.edu

***Abstract*— This paper presents the implementation of a grid connected photovoltaic system with harmonic compensation. Using only one dc-ac converter in photovoltaic energy conversion process, the system presents increased efficiency when compared to the conventional systems, composed by a dc-dc converter and a dc-ac converter. The system can be controlled for current harmonics and reactive power compensations simultaneously by using the converter also operating as active shunt filter. The synchronous reference frame method is chosen to control the converter and experimental results, corresponding to the operation of the photovoltaic system controlled by digital signal processor, are presented.**

***Keywords* - Converter control, Power Quality, Renewable energy systems, Solar Cell Systems, Vector control.**

I. INTRODUCTION

In Brazil, the main energy resource is the hydraulic and it has the advantage of not introducing harmful substances or products into the environment, but the ambient impact is significant. A study made by the Universidade de São Paulo and the Greenpeace suggests the use of new energy resources to decrease the harmful substances in the air. This study shows that in 2,050 the energy electric utilization would be four times higher than today and in according to specialists this situation would be inviable. Therefore, the purpose would be to increase the use of renewable energies. The projection for 2,050 is that the solar energy participates with 4% of the renewable energies in Brazil. However, the participation of the solar energy in Brazil can be higher with the improvement of the Photovoltaic (PV) cell. In the conventional cells used today, the efficiency is only 22%. The American Company Spectrolab is testing a PV cell of concentrated light capable of transforming in electricity 40.7% of the solar rays that reach it. This means that this technology is twice more efficient and it can be the first step of a revolution in the energy business. Companies equipped with this technology will generate electricity from 8 to 10 cents of dollar per quilowatt/hora, that it is almost the same of the energy generated by termelectric utilities.

A way of using PV energy is in a system of distributed energy as an auxiliary energy resource. This system utilizes a high number of photovoltaic panels and it does not have energy storage because all generation is delivered to the grid. All array is connected to converters that act as interface element between the panel and the grid, to adequate the dc waveforms from the panel to the ac waveforms needed to connect to the grid. These converters must satisfy the exigences of quality and safety in such a way that the grid does not be affected.

Strict regulations have been applied to equipment connected to the grid. Some of these regulations are related to harmonics distortion and power factor [1]. Passive filters have been traditionally used to absorb harmonic generated by nonlinear loads. They have the advantage of being simple and cheap. However, the passive filters have some problems like resonance that discourage their use [2][3]. With the advent of fast commutating switches, the Active Filter (AF) appeared as a better way to eliminate harmonics related problems and it is becoming a cost effective solution [4][5]. The shunt AF was the first AF alternative to mitigate harmonics problems [4]. The approach is based on the injection of harmonics currents into the ac system, of the same amplitude and reverse phase of the load current harmonics [6][7].

On the other hand, the rising complexity of power electronics applications and their control techniques require an increasing use of microcontrollers and Digital Signal Processors (DSP). The DSP is a device that manipulates digital data with the objective of generating control signals in real time. With the recent advance of technology, the use of DSP have becoming cost competitive and it will be only a matter of time for these chips totally replace the conventional analog control circuits.

The purpose of this paper is to present a PV system with harmonic compensation for connection in a three-phase grid. The system provides the functions of current harmonic and reactive power compensations. A DSP is used to implement the control of the system using the Synchronous Reference Frame (SRF) method.

II. MAXIMUM POWER POINT TRACKING

The PV cell has the equivalent circuit shown in Fig. 1. Considering that R_P (the PV cell shunt resistance) is very large, the characteristic of a PV cell is given by [8][9]:

$$I_{PV} = I_g - I_o \left[\exp\left(\frac{q}{AkT}(V_{PV} - I_{PV}R_S)\right) - 1\right] \quad (1)$$

where I_{PV} is the PV cell output current, V_{PV} is the PV cell output voltage, I_g is the generated current under a given irradiance, I_o is the reverse saturation current, q is the charge of an electron, A is the ideality factor for a p-n junction, k

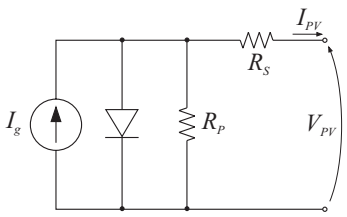

Fig. 1: Equivalent circuit of the PV cell.

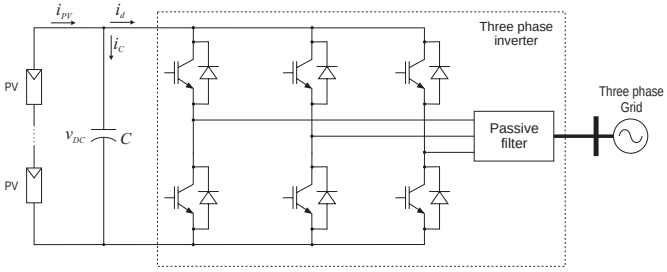

Fig. 2: Grid connected PV system.

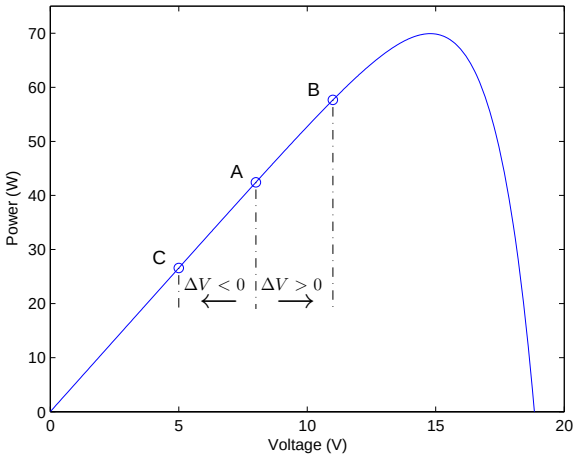

Fig. 3: Characteristic of the output power of the PV module for $S = 1000W/m^2$ and $T = 50^0C$.

is the Boltzmann's constant, T is the temperature and R_S is the PV cell series resistance.

The currents I_o and I_g of the PV cell change with temperature in according to [10]:

$$I_o = I_{or} \left[\frac{T}{T_r} \right]^3 exp \left[\frac{qE_{G0}}{kT} \left(\frac{1}{T_r} - \frac{1}{T} \right) \right] \quad (2)$$

$$I_g = \left[I_{scr} + K_I \left(T - T_r \right) \right] \frac{S}{S_r} \quad (3)$$

where I_{or} is the saturation current at T_r, T_r is the reference temperature, E_{GO} is the band-gap energy of the semiconductor used in cell, I_{scr} is the short-circuit current at T_r and S_r, S_r is the reference irradiance, K_I is the short-circuit current temperature coefficient and S is the irradiance.

The same model presented for the PV cell can be used for PV array, being necessary some modifications in the output current equation. Considering n_p the number of parallel connections and n_s the number of series connections of the PV array, the following modification in (1) must be done:

$$I = n_p I_g - n_p I_o \left[\exp\left(\frac{q}{AkT} \frac{V - IR_S}{n_s} \right) - 1 \right] \quad (4)$$

where I is the PV array output current, V is the PV array output voltage.

The study is for a grid connected PV system (Fig. 2) using a 1,848W PV array consisting of twenty four modules $MSX77$ connected is series. Each PV module has a maximum power rating of 77W, which occurs at a rated voltage of 16.9V and a rated current of 4.56A at $S = 1,000W/m^2$ and $T = 25^0C$. The modules have an open circuit voltage of 21V and a short circuit current of 5A for the same conditions. The grid connected PV system was tested in simulation by using Matlab. The cells were modeled by using equations (1), (2) and (3).

A. *Perturbation and Observation*

The Perturbation and Observation (P&O) technique compares the power of the previous step with the power of the new step in such a way that it can increase or decrease the voltage or current. This method changes the reference value by a constant factor of current or voltage. It moves the operating point toward the Maximum Power Point (MPP) by periodically increasing or decreasing the array voltage or current. The P&O method works well when the irradiance does not vary quickly with time. However, with this method the power oscillates around the MPP in steady state operation and it is not good when there are fast variations of irradiance.

From Fig. 3, it can be seen that incrementing (decrementing) the voltage increases (decreases) the power when operating on the left of the MPP and decreases (increases) the power when on the right of the MPP. Therefore, if there is an increase in power, the subsequent perturbation should be kept the same to reach the MPP and if there is a decrease in power, the perturbation should be reversed. A choice of high values of perturbation (ΔV) provides a fast tracking for the MPP voltage. If the perturbation has low value, the MPP Tracking (MPPT) is slower, but it has small oscillations around the MPP.

B. *Incremental Conductance Technique*

In the Incremental Conductance (IncCond) technique [11][12], the slope of power versus voltage characteristic is used (Fig. 3) [11]. It can be identified in which point of the curve the PV array voltage must be adjusted to reach the MPP voltage. The equation in the MPP is:

$$\frac{dP}{dV} = 0 \quad (5)$$

Or, it can be expressed as:

$$\frac{dP}{dV} = \frac{d(IV)}{dV} = I + V\frac{dI}{dV} = 0 \quad (6)$$

Hence, the array PV voltage can be adjusted to the MPP voltage by measuring the incremental and instantaneous array conductance (dI/dV and I/V, respectively). When $dP/dV < 0$, decreasing the reference voltage forces dP/dV to approach zero; when $dP/dV > 0$, increasing the reference voltage forces dP/dV to approach zero; when $dP/dV = 0$,

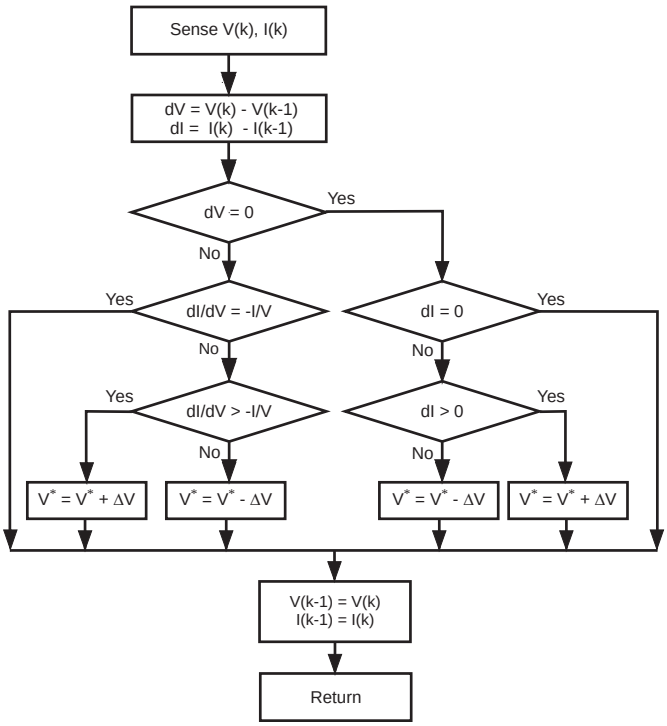

Fig. 4: The flowchart of the IncCond technique.

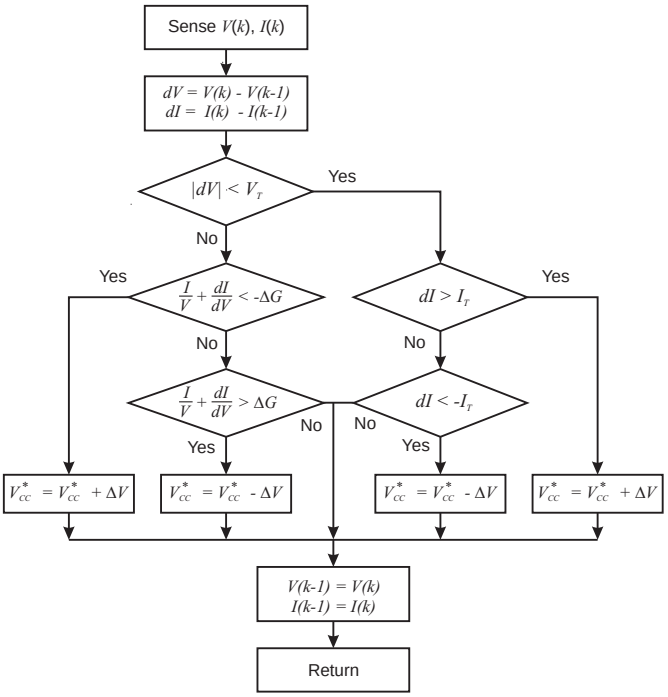

Fig. 5: The modified flowchart of the IncCond technique.

TABLE I: Efficiencies of the P&O and IncCond techniques with $T = 50^0C$ and $T_{MPPT} = 4\tau_{vcc}$

Irradiance conditions	P&O		IncCond
	$\Delta V = 2.5V$	$\Delta V = 1.0V$	$\Delta V = 1.0V$
$S = 500W/m^2$	99.9871 %	99.9981 %	99.9997 %
$S = 1,000W/m^2$	99.9884 %	99.9983 %	99.9998 %

reference voltage does not need any change. The flowchart is shown in Fig. 4.

Due to the measurement noises and mainly to the discrete process of the reference voltage, the condition $\frac{I}{V} + \frac{dI}{dV} = 0$ usually will not be achieved. A practical aspect is considering that the condition is true when it is between a tolerable range (ΔG) around zero ($-\frac{\Delta G}{2} < \frac{I}{V} + \frac{dI}{dV} < \frac{\Delta G}{2}$). Similar problems occur for the other comparisons in the technique, $dV = 0$ and $dI = 0$. The solution is the same, substituting zero by tolerable ranges. Therefore, the technique is modified to have the flowchart shown in Fig. 5.

C. Comparison between P&O and IncCond Techniques

To confirm the capacity of the techniques extract the maximum available power in the PV array, two steady state conditions $500W/m^2$ and $1000W/m^2$ are shown in Table I. The efficiency of the MPPT techniques are obtained by:

$$\eta_{MPPT} = \frac{\frac{1}{T_{vdc}}\int_0^{T_{vdc}} Pdt}{\frac{1}{T_{vdc}}\int_0^{T_{vdc}} P_{MPP}dt} = \frac{\int_0^{T_{vdc}} Pdt}{V_{MPP}I_{MPP}T_{vdc}}, \quad (7)$$

where T_{vdc} is the reference voltage period.

The comparison of efficiency for P&O and IncCond techniques in Table I shows that these techniques present similar efficiencies with the IncCond being a little better.

Even in steady-state, the reference voltage in the P&O technique oscillates around V_{MPP}. These oscillations also appear in i_d (Fig. 2). The currents that the PV system injects in the grid are function of i_d that can be obtained by the Park transformation, meaning that the currents injected in the grid will be distorted. Figure 6 shows the reference voltages and the grid currents in phase a obtained by the P&O and IncCond techniques for a steady-state condition. In the P&O technique, the grid currents are distorted, having low power quality. When i_{PV} is much higher than the i_d variation, this effect is neglected. However, in many cases i_{PV} and i_d variation will have similar amplitudes. To decrease the distortion, a low value for the proportional gain in the control loop can be used, but the converter dynamics will be slower. This dynamics implies in higher tracking time. Due to these aspects, the IncCond technique is chosen as the best technique to be implemented in the prototype.

D. Experimental Results

The experimental results were obtained by using power measurements in the real ambient conditions. The grid connected PV system shown in Fig. 2 is used to validate the simulation results with the following procedure: from 0 to 7.5s, the reference voltage is linearly incremented to build the PV array power curve. From 7.5s to 50s, a MPPT method is used to track the maximum power point. Simulation and experimental results for Perturbation and Observation (P&O) and IncCond methods are shown in figures 7 and 8, respectively. In these figures, the average power in simulation is around 1489W and it was verified by using a irradiance measurement that the irradiance was constant during the data acquisition process. It can be seen a very good agreement between simulation and experiment, showing that the PV

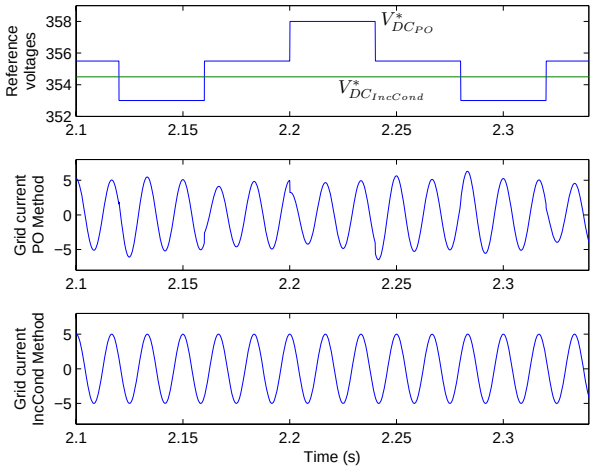

Fig. 6: Grid currents using the P&O and IncCond techniques

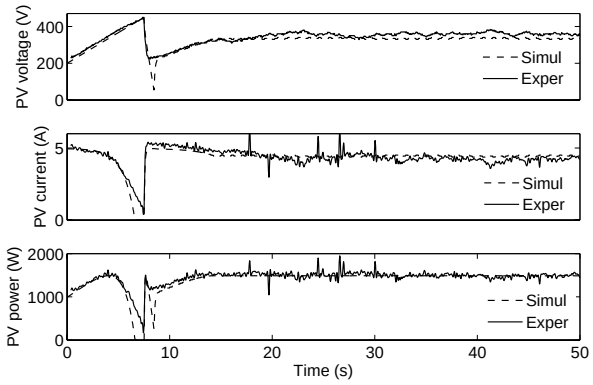

Fig. 7: Simulation and experimental results for PO method.

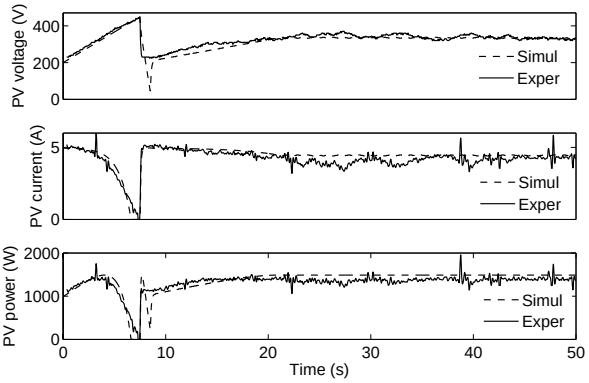

Fig. 8: Simulation and experimental results for IncCond method.

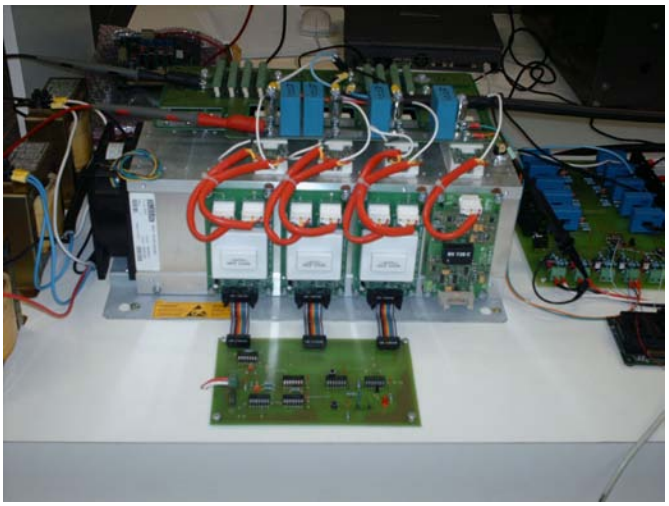

Fig. 9: Picture of the experimental system.

array model used in simulations is valid.

The experimental results were obtained for a grid connected PV system using a 1,848W PV array consisting of twenty four modules $MSX77$ connected is series. The prototype of the system is composed of a converter (this converter is also used as the shunt active filter) plus an output filter, a capacitor set (dc link). Figure 9 shows the picture of the experimental system. For the experimental results shown in this paper, the parameters of the system are: line-to-line rms voltage 110V, output filter inductor (1.8mH, 10A), inverter with 6 switch + diode (1200V, 50A), dc-link capacitor (7mF, 900V).

The implementation of the system is done using a DSP to process the control algorithm and generates the PWM pulses. The current and voltage signals are sensed using Hall-effect sensors and instrumentation amplifiers. This acquisition system was built to decrease the amplitude of the signal references to a range between zero and 3 volts and the output signals have the additional characteristic of a low output impedance with the objective of wasting as little time as possible in the analogue-digital conversion. A DSP is a specific device to manipulate digital data that are measured by analogue-digital converters with the objective of processing these data as quickly as possible to generate output signals to control systems in real time operation.

The TMS320F2812 used to implement the control system can be classified as Digital Signal Controller (DSC). Combining the computational capacity of DSP with memory and peripherals like analogue-digital converters and event managers in one single device, it is possible to have an effective solution on digital control in real-time. In a general way the DSC can be considered a DSP device. The DSP TMS320F2812 used in the implementation of the control system was a fixed-point DSP with capacity of processing 150 millions of information per second using fixed-point with words of 32 bits. All operations in the control strategy are done in Q.22 notation. The architecture of this kind of DSP is based on Harvard architecture, so two independent buses systems exist: one for the program memory and other for data memory. Hence it facilitates the access to the memory map, decreasing the time to access the memory. The memory space is divided in program and data space. There are different types of memory: flash, RAM (SARAM), expanded SARAM and boot ROM memory.

For the implementation of the control system it is necessary to use 8 of 16 channels of the analog to digital conversion module. Each signal spends at least 200ns to be converted. The analog to digital conversion module has resolution of

12 bits and it was configured in cascaded mode, which means that all channels were converted one by one and once a conversion is completed, the selected channel value is stored in the respective result register. Once the analogue-digital conversion is concluded, a low-pass finite impulse response filter is used to separate the harmonics from the fundamental component of the load current for compensating current harmonics and reactive power. This filtering is done using the dq components, in such way that it is only needed to filter the dc component of the signal with a cutoff frequency of approximately 20Hz. The SRF-based controller is strongly influenced by the Phased Locked Loop (PLL) performance. The SRF method can be improved if the characteristics of the PLL are changed.

The switching frequency of the system is 20KHz and a counter with an interrupt routine was used to give a basis of time to impose this frequency. It means that in each $50\mu s$, the output registers of DSP need to be changed. The event manager is responsible for the generation of this basis of time to calculate the switches duty cycle. This peripheral is able to produce hardware signals directly from an internal time event. The interrupt system of DSP consists of 16 types of interrupts; two of them are non-maskable and 14 are maskable. Each 16 types of interrupts have different priorities. The interrupt called ADCINT (maskable hardware interrupt) was used to impose the frequency to the system. This routine is always initialized in the end of the last signal conversion and a counter called TxCNT is responsible for making sure that the analogue-digital conversion will be started at each $50\mu s$.

III. PLL INFLUENCE ON THE SYSTEM RESULTS

The PLL of Fig.10, used in SRF method, called SRF-PLL, under undistorted and balanced supply voltage yields to good results. However, under distorted and/or unbalanced supply voltage, the angle in the output of SRF-PLL can not be correctly estimated. The experimental results were obtained by simulating a short-circuit in one phase, having the effect of a voltage sag at the point of connection of the PV system in phase *b* (Fig. 11). The voltage sag in only one phase makes the system have negative sequence voltage. The high bandwidth of the SRF-PLL increases the problems related to voltages unbalance. To reduce the effects of this unbalance, the PLL bandwidth can be reduced [13]. The SRF-PLL experimental response for two different bandwidth are shown in Fig.12 and Fig.13. It can be seen that the phase angle from the SRF-PLL reference angle in Fig. 12 presents lower distortion than the phase angle in Fig. 13. The first case (Fig. 12) was an experiment with a low bandwidth and the second case (Fig. 13) was an experiment with a high bandwidth. The J-TAG peripheral allows watching variables while the code is running in real-time, without any delay to the control code. Figures 11- 13 were captured using J-TAG peripheral.

The SRF-PLL has some limitations: the true amplitude of the positive sequence component is not detected, the dynamic response of the system is very poor and under unbalanced supply voltage the PLL response is not good as is shown in [14].

The PLL proposed in [14] is called Double Synchronous Reference Frame PLL (DSRF-PLL) and in this paper it is

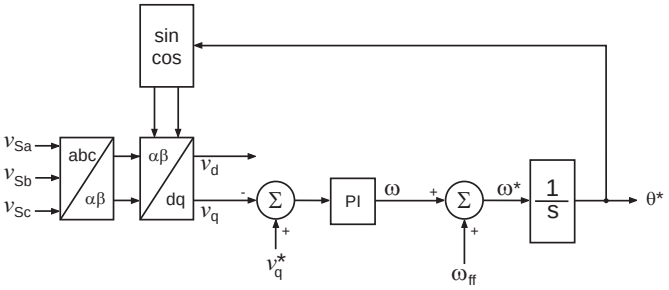

Fig. 10: SRF-PLL scheme for SRF-based controller.

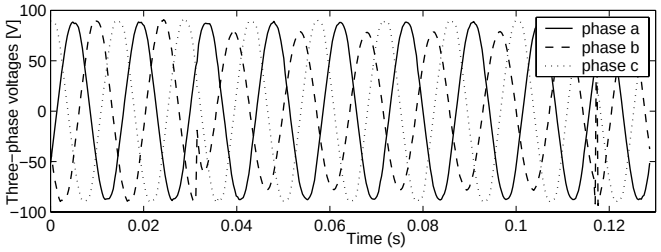

Fig. 11: Experimental three-phase grid voltages.

implemented to be experimentally compared with the SRF-PLL. With the DSRF-PLL is possible to get the positive sequence reference v_d^{+1} required to implement this reference extraction strategy. The control loop bandwidth of the DSRF-PLL can be increased in relation to the SRF-PLL and the amplitude of the positive sequence voltage component can be detected accurately. The principle of DSRF-PLL is decouple the positive and negative sequence of a voltage vector. It is supposed that a vector consisting of two generic components is rotating with $n\omega$ and $m\omega$ frequencies respectively, where n and m can be the positive and negative sequence +1 and -1. It will be considered two rotating reference frames, dq^n and dq^m, whose angular positions are $n\theta'$ and $m\theta'$, being θ' the phase angle of PLL (Fig. 14).

The amplitude of the signal oscillating in the dq^n depends

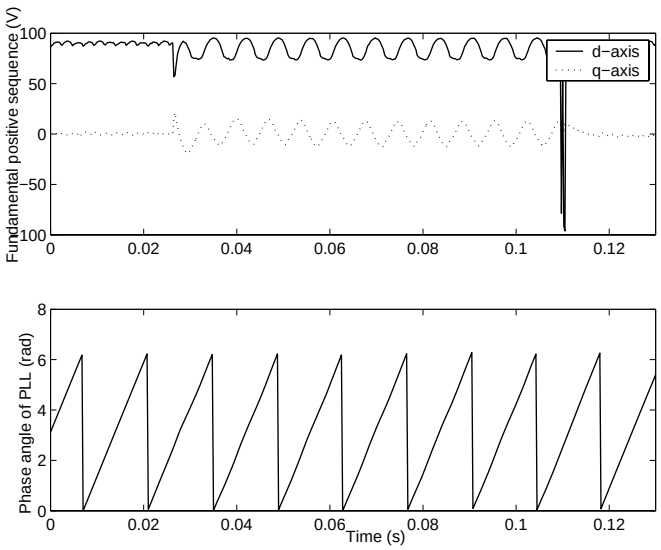

Fig. 12: Experimental results for the SRF-PLL with low bandwidth.

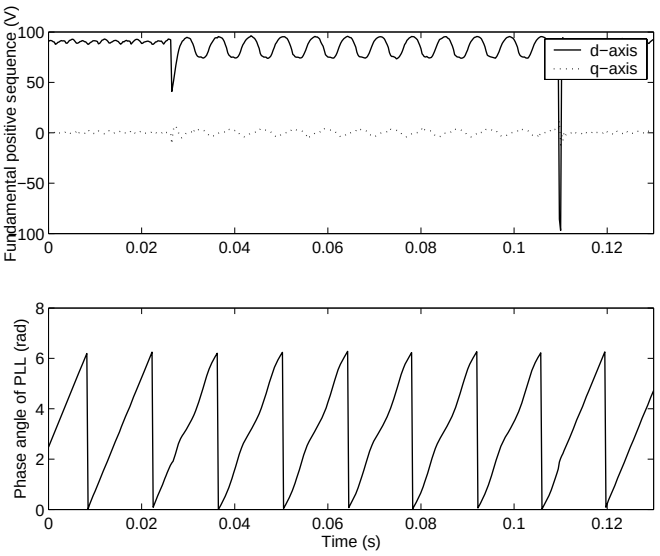

Fig. 13: Experimental results for the SRF-PLL with high bandwidth.

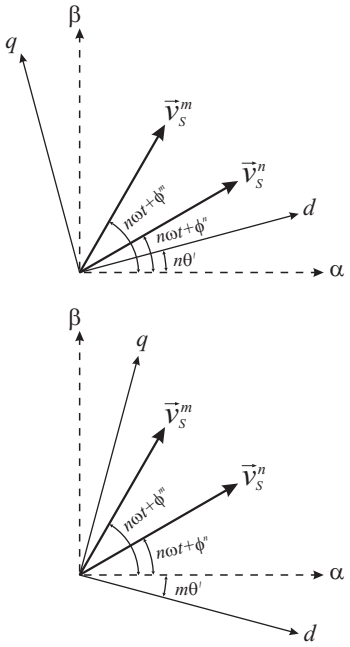

Fig. 14: Voltages vectors and axis $d^n - q^n$ and $d^m - q^m$.

on the mean value of the signal in the dq^m axis, and vice versa. The decoupling cell is shown in Fig.15. In the Fig.16 is shown the block diagram of DSRF-PLL where $n = +1$ and $m = -1$. The decoupling cell can be used to mitigate the influence of some harmonic as done in [14]. Considering the scheme to prevent the negative sequence in the obtention of the angle it is possible to find the experimental results of Fig. 17. The voltage sag in only one phase makes the system have negative sequence voltage as shown in Fig. 17. The correct angle capture makes possible the recovery of voltages with a unbalanced supply voltage.

IV. PV SYSTEM WITH ACTIVE FILTER FUNCTION

In the grid connected PV system with active filter function (Fig. 18), when the sun is available the inverter operates converting the energy from the PV array as well as compensating

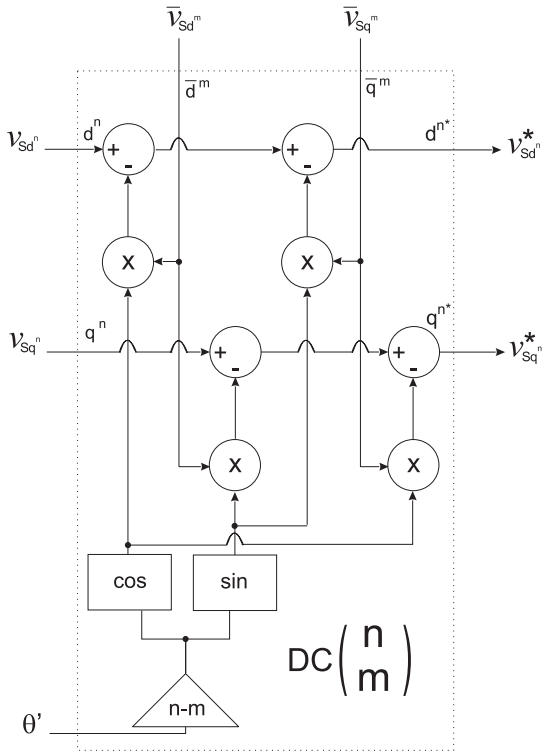

Fig. 15: Decoupling cell.

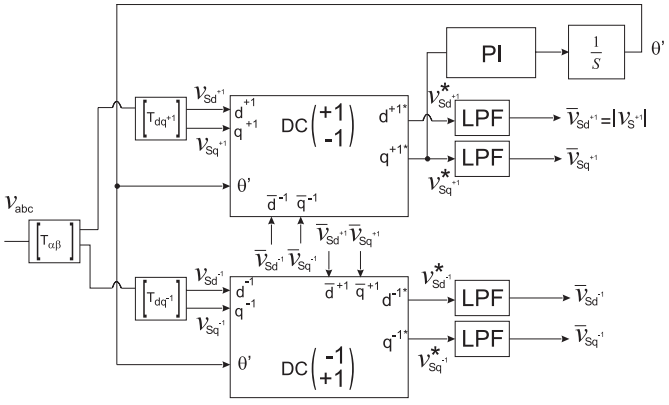

Fig. 16: Block diagram of PLL.

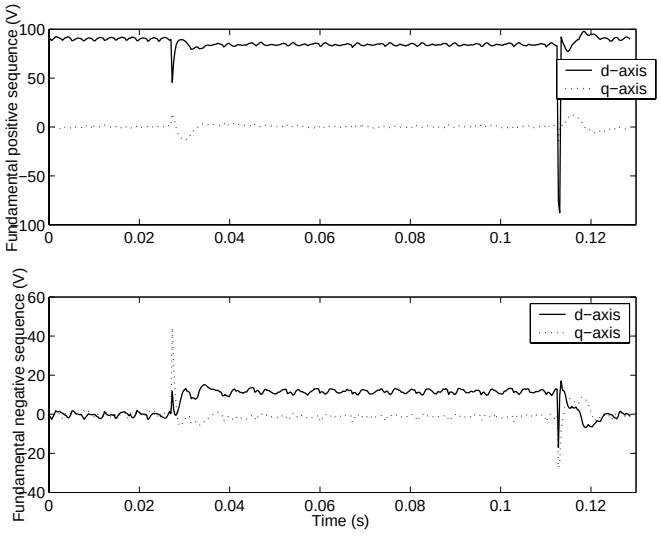

Fig. 17: DSRF-PLL: fundamental positive and negative sequences.

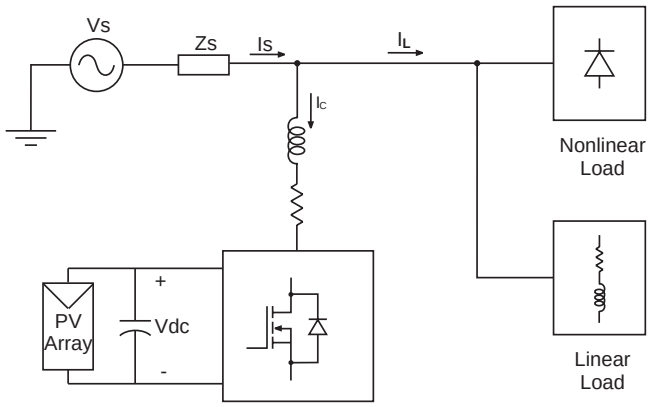

Fig. 18: PV generation with AF function.

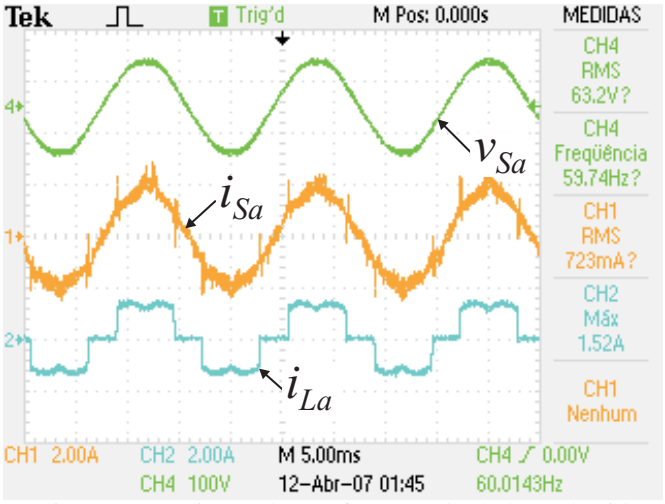

Fig. 19: Experimental waveforms under balanced grid voltage without PV generation: nonlinear load.

harmonic and reactive power. The IncCond method keeps the maximum power in the PV array and the controller can compensate harmonic and reactive power effectively as shown in figures 19-25. In figures 19-25 the grid voltage, the grid current and the load current in phase *a* are shown from top to bottom. Figures 19-23 were obtained under undistorted and balanced grid voltage. Figures 24 and 25 were obtained by simulating a short-circuit in one phase, having the effect of a voltage sag at the point of connection of the PV system in phase *b*. Figures 21, 23 and 25 show that the grid current is displaced by 180 degrees from the grid voltage because it is generated more power from the PV array than that needed for the load. Therefore, in this case the PV array supplies the load and injects power for the grid. When the sun is not available, the system operates only as harmonics and reactive power compensator (figures 19, 22 and 24). In this case, the grid current is in phase with the grid voltage showing that the load is supplied by the grid.

V. CONCLUSION

The topology implemented in this paper improves functionality in grid connected photovoltaic generation systems. The excellent performance of the system is verified from simulation and experimental results. The voltage waveform in the photovoltaic array follows the reference voltage for

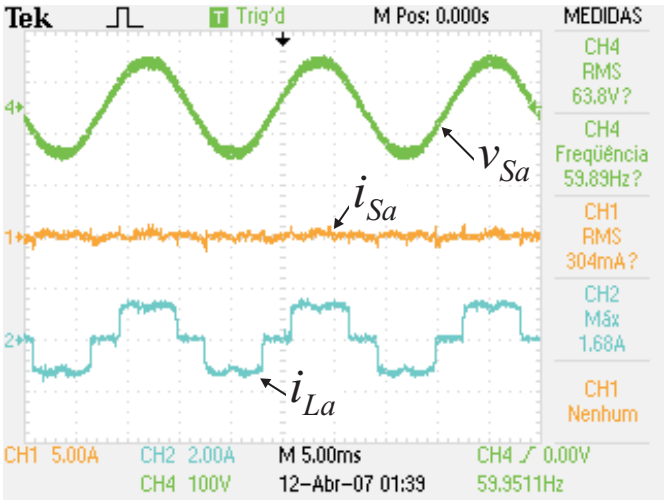

Fig. 20: Experimental waveforms under balanced grid voltage with PV generation and low irradiance: nonlinear load.

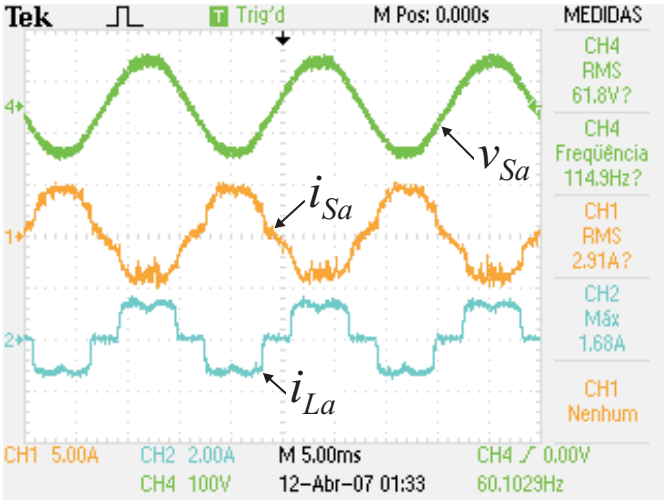

Fig. 21: Experimental waveforms under balanced grid voltage with PV generation and high irradiance: nonlinear load.

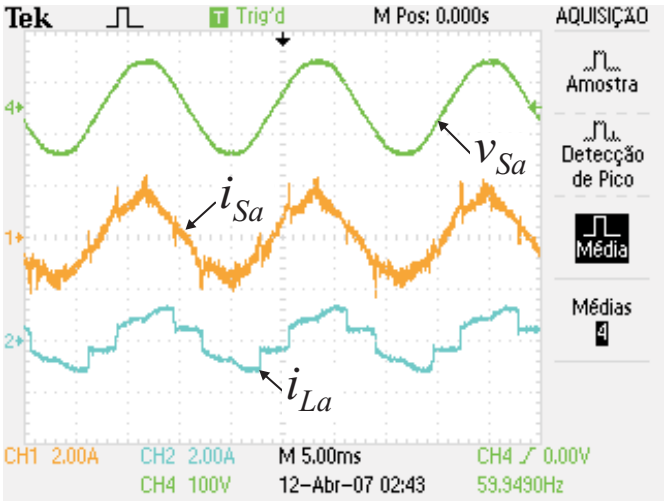

Fig. 22: Experimental waveforms under balanced grid voltage without PV generation: nonlinear and linear loads.

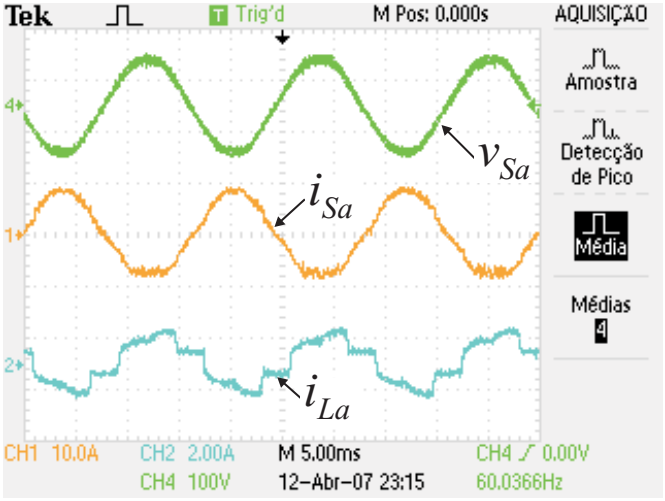

Fig. 23: Experimental waveforms under balanced grid voltage with PV generation and high irradiance: nonlinear and linear loads.

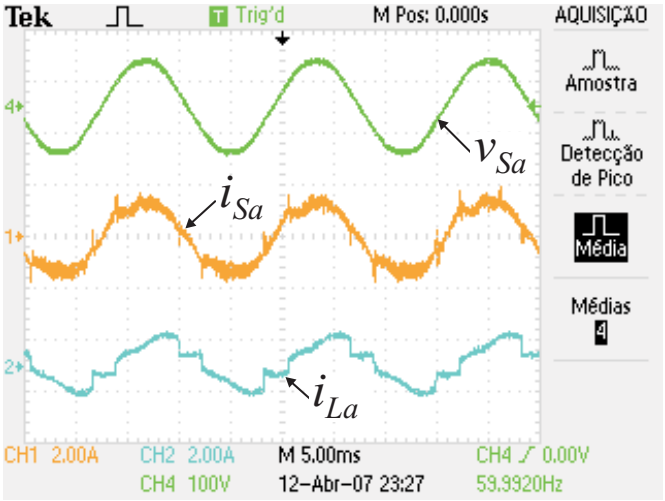

Fig. 24: Experimental waveforms under unbalanced grid voltage without PV generation: nonlinear and linear loads.

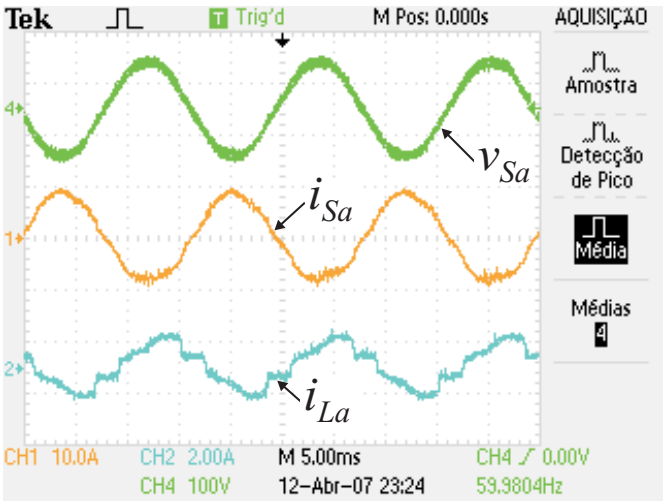

Fig. 25: Experimental waveforms under unbalanced grid voltage with PV generation and high irradiance: nonlinear and linear loads.

all irradiation conditions. Besides that, the controller also compensates current harmonics and reactive power. The use of digital signal processors, with the recent advance of technology, has becoming cost competitive and it will be only a matter of time for these chips totally replace the conventional analog control circuits.

REFERENCES

[1] Roger C. Dugan, Mark F. McGranagham, Surya Santoso e H. Wayne Beaty. d *"Electrical Power Systems Quality"*,McGraw-Hill, Second edition.

[2] F.Z. Peng, H. Akagi and A. Nabae, *"A Novel Harmonic Power Filter"*, IEEE/PESC pp 1151-1158, 1988.

[3] S. Bhattacharya and D. Divan *"Synchronous Frame Based Controller Implementation for a Hybrid Series Active Filter system"*, in Conf. Rec. IEEE-IAS Annu. Meeting, pp 2531-2540, 1995.

[4] Hirofumi Akagi *"New Trends in Active Filters for Power Conditioners"*, IEEE/Trans. Trans on Industry appl. No 6, Vol 32 pp 1312-1322, 1996.

[5] B.Singh, K. Al-Haddad and A. Chandra *"A Review of Active Filters for Power Quality Improvement"*, IEEE/Trans. Ind. Elect. No 5, Vol 46 pp 960-971, 1999.

[6] S. Bhattacharya, T. M. Frank, D.M. Divan and B. Banerjee. d *"Active filter System Implementation"*, IEEE Ind. Appl. Magazine Vol 4, Issue 5 pp 47-63 , 1998.

[7] Maurício Aredes *"Active Power Line Conditioners "*, Doctorate Thesis, Tecnhical university of Berlin, 1996.

[8] C. Hua and C. Shen, *Comparative study of peak power tracking techniques for solar storage systems*, IEEE Applied Power Electronics Conference and Exposition, pp. 679-685, 1998.

[9] Y. C. Kuo, T. J. Liang, and J. F. Chen, *A high-efficiency single-phase three-wire photovoltaic energy conversion system*, IEEE Trans. on Industrial Electronics, vol. 50, no. 1, pp. 116-122, February 2003.

[10] G. J. Yu, Y. S. Jung, J. Y. Choi, I. Choy, J. H. Song, and G. S. Kim, *A novel two-mode MPPT control algorithm based on comparative study of existing algorithms*, IEEE Photovoltaic Specialists Conference, pp. 1531-1534, 2002.

[11] K. H. Hussein, I. Muta, T. Hoshino, and M. Osakada, *Maximum photovoltaic power tracking: an algorithm for rapidly changing atmospheric conditions*, IEE Proc. Generation, Transmission and Distribution, vol. 142, pp. 59-64, Jan. 1995.

[12] T. Y. Kim, H. G. Ahn, S. K. Park, and Y. K. Lee, *A novel maximum power point tracking control for photovoltaic power system under rapidly changing solar radiation*, IEEE International Symposium on Industrial Electronics, pp. 1011-1014, 2001.

[13] V. Kaura and V. Blasko *"Operation of a Phase Locked Loop System Under Distorted Utility Conditions"*, Trans. Ind. Applic. Vol 33, No 1, pp 58-63, 1997.

[14] P. Rodriguez, J. Pou, J. Bergas, I. Candela, R. Burgos, D. Boroyevic *"Double Synchronous Reference Frame PLL for Power Converters Control"*, Power Electronics Specialists, 2005 IEEE 36th Conference on June 12, pp: 1415 - 1421, 2005.